ELSEVIER

Available online at www.sciencedirect.com

ScienceDirect

Coordination Chemistry Reviews 251 (2007) 2537–2546

COORDINATION CHEMISTRY REVIEWS

www.elsevier.com/locate/ccr

Review

Design and syntheses of nano-structured ionic crystals with selective sorption properties

Sayaka Uchida, Noritaka Mizuno*

Department of Applied Chemistry, School of Engineering, The University of Tokyo, 7-3-1 Hongo, Bunkyo-ku, Tokyo 113-8656, Japan

Received 28 December 2006; accepted 21 February 2007
Available online 1 March 2007

Contents

Abstract

This review describes the design and syntheses of nano-structured ionic crystals with selective sorption properties. The complexation of Keggin-type polyoxometalates of $[\alpha\text{-}XW_{12}O_{40}]^{n-}$ ($n = 3$–6) with a macrocation of $[Cr_3O(OOC\mathit{H})_6(H_2O)_3]^+$ and alkali metal ions forms ionic crystals with hydrophilic channels. The ionic crystals can recognize small polar molecules such as alcohols, nitriles, and esters by the difference of one methylene chain. On the other hand, the use of a macrocation of $[Cr_3O(OOC\mathit{C_2H_5})_6(H_2O)_3]^+$ forms both hydrophilic and hydrophobic channels in the ionic crystals, and the channel-selective sorption and collection of hydrophilic and hydrophobic molecules has been successfully carried out.

Keywords: Ionic crystals; Polyoxometalates; Macrocation; Selective sorption

1. Introduction

Crystalline solids with molecular-sized spaces have attracted the attention of chemists because of their interests in the unique guest sorption, ion exchange, and catalytic properties. These solids can be classified into three groups by the kinds of chemical bonds, which construct the framework: (i) inorganic zeolites (covalent bonds) [1–5]; (ii) metal organic frameworks or coordination polymers (coordination bonds) [6–10]; (iii) layered compounds and ionic crystals (hydrogen bonds and/or ionic bonds) [11–13]. Inorganic zeolites are composed of covalently bonded $[TO_4]$ (T = Si, Al, P, etc.) and $[MO_6]$ (M = Ti, Zr, Sn, etc.) units, contain stable nano-sized pores (ca. 3–15 Å), and show the molecular sieving effects depending on the framework geometry and pore size. A classical example is a Ca–A zeolite, which possesses eight-membered ring and pore size of 5 Å, and adsorbs straight-chain organic molecules but not those that are branched [5]. As for the separation of inorganic gases, the titanosilicate, of which the effective pore size can be finely tuned by the dehydration at elevated temperatures, can separate 3–4 Å molecules such as N_2/CH_4, Ar/O_2, and N_2/O_2 with the pressure-swing adsorption [3]. Recently, much attention has been paid

---

* Corresponding author. Tel.: +81 3 5841 7272; fax: +81 3 5841 7220.
E-mail address: tmizuno@mail.ecc.u-tokyo.ac.jp (N. Mizuno).

0010-8545/$ – see front matter © 2007 Elsevier B.V. All rights reserved.
doi:10.1016/j.ccr.2007.02.019

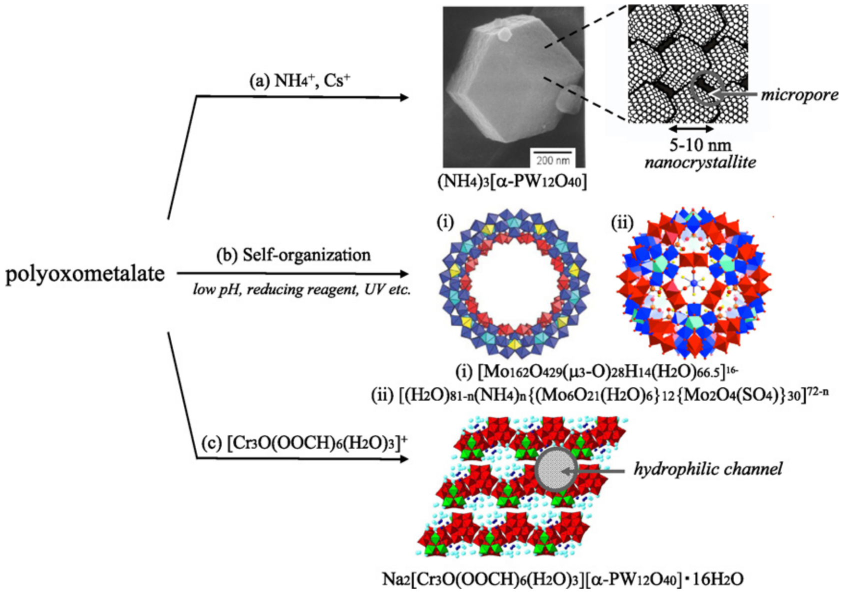

Fig. 1. Classification of porous polyoxometalate compounds: (a) NH_4^+; (b) self-organization; (c) $[Cr_3O(OOCH)_6(H_2O)_3]^+$.

toward the syntheses of metal organic frameworks or coordination polymers constructed with the coordination bonds between the metal and organic building units. The framework geometry, pore surface, and guest sorption properties can be finely tuned by the choice of building blocks. For example, Yaghi and co-workers have synthesized a series of metal-organic frameworks with zinc-benzenecarboxylates, and IRMOF-16 shows the highest free volume (91.1%) and the lowest density ($0.21\,g\,cm^{-3}$) among those reported for porous crystalline solids [14]. Kitagawa and co-workers have shown that acetylene molecules form arrays in the micropore of a copper coordination polymer by the hydrogen bonding with the pore surface. Stable storage of acetylene at a density of 200 times the safe compression limit of free acetylene at room temperature has been achieved [15]. Layered compounds such as montmorillonites and mixed-metal layered hydroxides possess cations or anions in the interlayer space and the layered structures are stabilized by the ionic bonds and hydrogen-bonds. The layered compounds swell in water and polar organic molecules with the expansion of the interlayer space [16]. Recently, the control of the porosity of ionic crystals such as metal carbonates and sulfates has been extensively attempted [13]. Since ionic bonds are formed by the strong Coulomb interactions between anions and cations, the bonds are isotropic and the ions are often densely packed in the crystal lattice. Therefore, pores exist mainly between the primary particles of ionic crystals, and the extent of porosity is controlled empirically by changing the degree of supersaturation of the synthetic solution [17].

Polyoxometalates, which are nano-sized metal-oxide macroanions and show unique redox or acidic properties, can create molecular-sized spaces within them or in the solid state with the combination of appropriate cations [18–26]. As shown in Fig. 1, porous polyoxometalate compounds can be classified into three groups with regard to the location of the pores; compounds with pores in (a) the intercrystallite space [27–29], (b) the molecular structure of polyoxometalates [30,31], and (c) the crystal lattice created by the arrangements of polyoxometalates and molecular cations (macrocations) [32–41]. The examples of (a)–(c) are described below.

As shown in Fig. 1a, $(NH_4)_3[\alpha\text{-}PW_{12}O_{40}]$ is non-porous single crystal when synthesized at 473 K, while submicron-sized dodecahedron particle form by the self-organization of 5–10 nm nanocrystallites at 368 K [28]. The crystallographic analysis of the single crystal shows that NH_4^+ and $[\alpha\text{-}PW_{12}O_{40}]^{3-}$ are closely packed in the crystal lattice, and no pores exist. On the other hand, the dodecahedron particle shows type-I N_2 adsoption isotherm characteristic of compounds with micropores. The surface area ($65\,m^2\,g^{-1}$) is larger than the outer surface area of the dodecahedron particle ($4\,m^2\,g^{-1}$), and the calculated crystallite size is 10 nm. The electron diffraction of the dodecahedron particle shows discrete spots, indicating that the nanocrystallites are crystallographically ordered in the particles. Therefore, it is probable that the $(NH_4)_3[\alpha\text{-}PW_{12}O_{40}]$ dodecahedron particle is formed by the self-organization of nanocrystallites and the micropores exist in the intercrystallite space.

As shown in Fig. 1b, ring shaped or spherical nano-sized polyoxometalate clusters are formed by the self-organization of several tens to more than hundred molybdenum atoms in acidic solution with reducing reagents [30] or under UV irradiation [31]. Water of crystallization exists in the ring or sphere, and a part of the water molecules can be exchanged with amphiphilic molecules such as methanol and formic acid.

The assembly of polyoxometalates (macroanions) and molecular cations (macrocations) can create ionic crystals with specific structures (Fig. 1c) [32–41]. By the control of the shape, size, and charge of the macroions, it is possible to predetermine their arrangement and to create molecular-sized spaces in the crystal lattice. The expected properties of the ionic crystals are summarized below: (i) while ionic crystals are usually dense and non-porous because of the strong and isotropic ionic bonds,

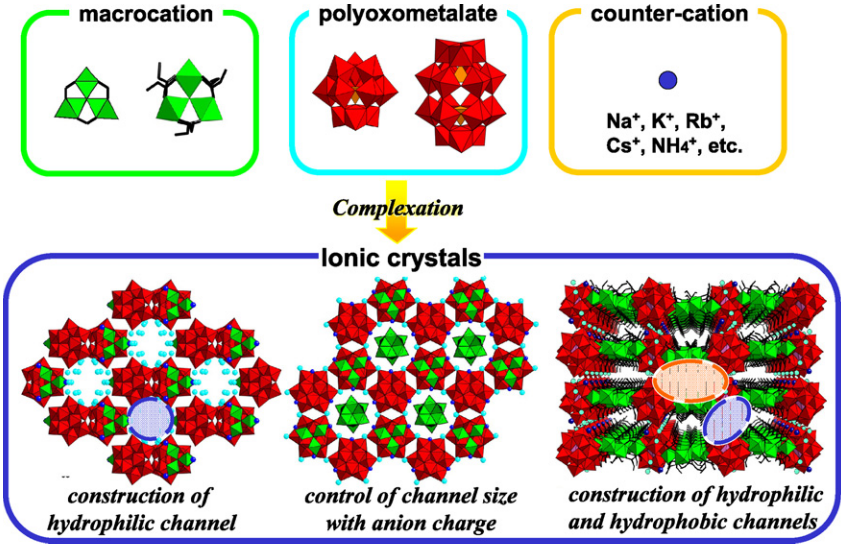

Fig. 2. Construction of ionic crystals.

the use of macroions would reduce the Coulomb interaction and enable the construction of space within the crystal lattice; (ii) ionic crystals formed by the complexation of inorganic polyoxometalate and organic macrocations are inorganic–organic hybrids and may show pore surface and guest sorption properties different form inorganic zeolites and organic coordination polymers; (iii) incorporation of catalytically active polyoxometalates will enable the heterogeneous catalysis in the crystal lattice. In the case of coordination polymers, there is difficulty in the creation of coordinatively unsaturated metal sites for the catalytic reaction, and the catalysis of coordination polymers remains largely unexplored.

As shown in Fig. 2, we have reported that (1) the complexation of Keggin-type polyoxometalates of $[\alpha\text{-XW}_{12}\text{O}_{40}]^{n-}$ ($n = 3$–6) with a macrocation of $[\text{Cr}_3\text{O(OOCH)}_6(\text{H}_2\text{O})_3]^+$ and alkali metal ions forms ionic crystals with hydrophilic channels. It is also demonstrated that (2) the channel sizes of ionic crystals of Dawson-type polyoxometalates of $[\alpha\text{-P}_2\text{V}_x\text{W}_{18-x}\text{O}_{62}]^{(6+x)-}$ increase with the decrease in x and can be controlled. While the use of a macrocation of $[\text{Cr}_3\text{O(OOC}H)_6(\text{H}_2\text{O})_3]^+$ forms only hydrophilic channels, (3) the use of a macrocation of $[\text{Cr}_3\text{O(OOC}C_2H_5)_6(\text{H}_2\text{O})_3]^+$ forms both hydrophobic and hydrophilic channels in the crystal lattice. In this review, our recent works on (1) and (3) are highlighted [42–49].

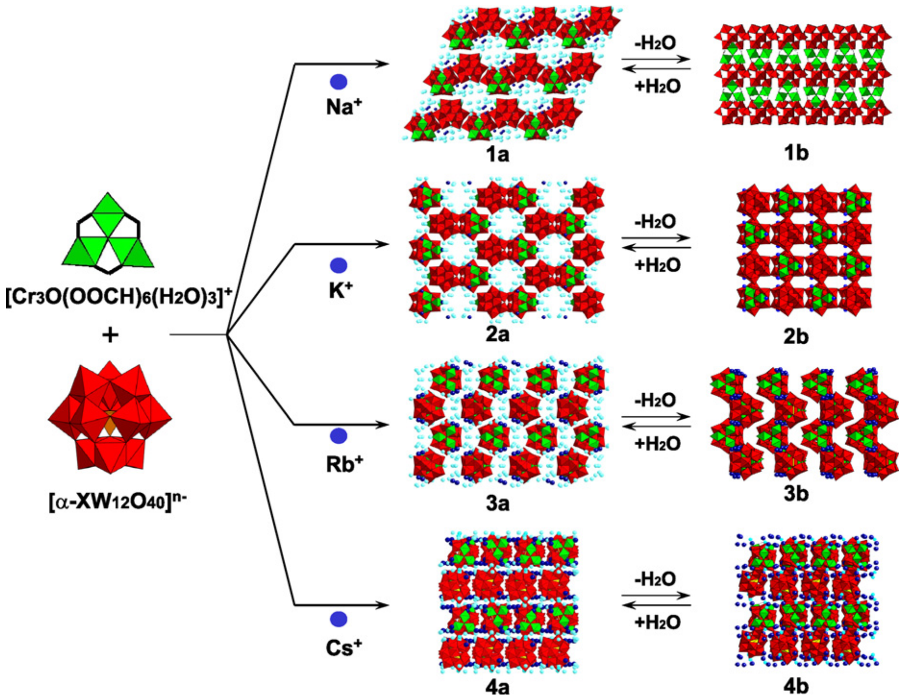

Fig. 3. Syntheses of ionic crystals with Keggin-type polyoxometalates of different anion charges.

2. Ionic crystals with hydrophilic channels and selective guest sorption

2.1. Syntheses and crystal structures

The schematic illustration of the syntheses and crystal structures of the compounds $Na_2[Cr_3O(OOCH)_6(H_2O)_3][\alpha\text{-}PW_{12}O_{40}]\cdot 16H_2O$ [**1a**], $K_3[Cr_3O(OOCH)_6(H_2O)_3][\alpha\text{-}SiW_{12}O_{40}]\cdot 16H_2O$ [**2a**], $Rb_4[Cr_3O(OOCH)_6(H_2O)_3][\alpha\text{-}BW_{12}O_{40}]\cdot 16H_2O$ [**3a**], and $Cs_5[Cr_3O(OOCH)_6(H_2O)_3][\alpha\text{-}CoW_{12}O_{40}]\cdot 7.5H_2O$ [**4a**] is shown in Fig. 3 [42,44,48]. Elemental analyses of **1a**–**4a** showed that the macrocation/polyoxometalate ratios were 1:1 and the stoichiometry in the complexes formed did not change among **1a**–**4a**, while the macrocation/polyoxometalate ratio in the synthetic solution was varied. The surplus anion charge was neutralized by the alkali metal ions. The polyoxometalates and macrocations lined up alternately to form columns, which were arranged in a honeycomb (**1a**, **2a**) or layered structure (**3a**), or densely packed (**4a**). The distance between the carbon atoms of the bridging formates in the macrocations and the oxygen atoms of the polyoxometalates in the same column were in hydrogen-bonding distances (C–H···O distances were 3.25–3.37, 3.09–3.27, 2.79–3.06, and 2.81–3.07 Å for **1a**–**4a**, respectively). The spaces between the columns were occupied with the water of crystallization and the space volumes for **1a**–**4a** corresponded to 36%, 36%, 32%, and 17% of the crystal lattices, respectively.

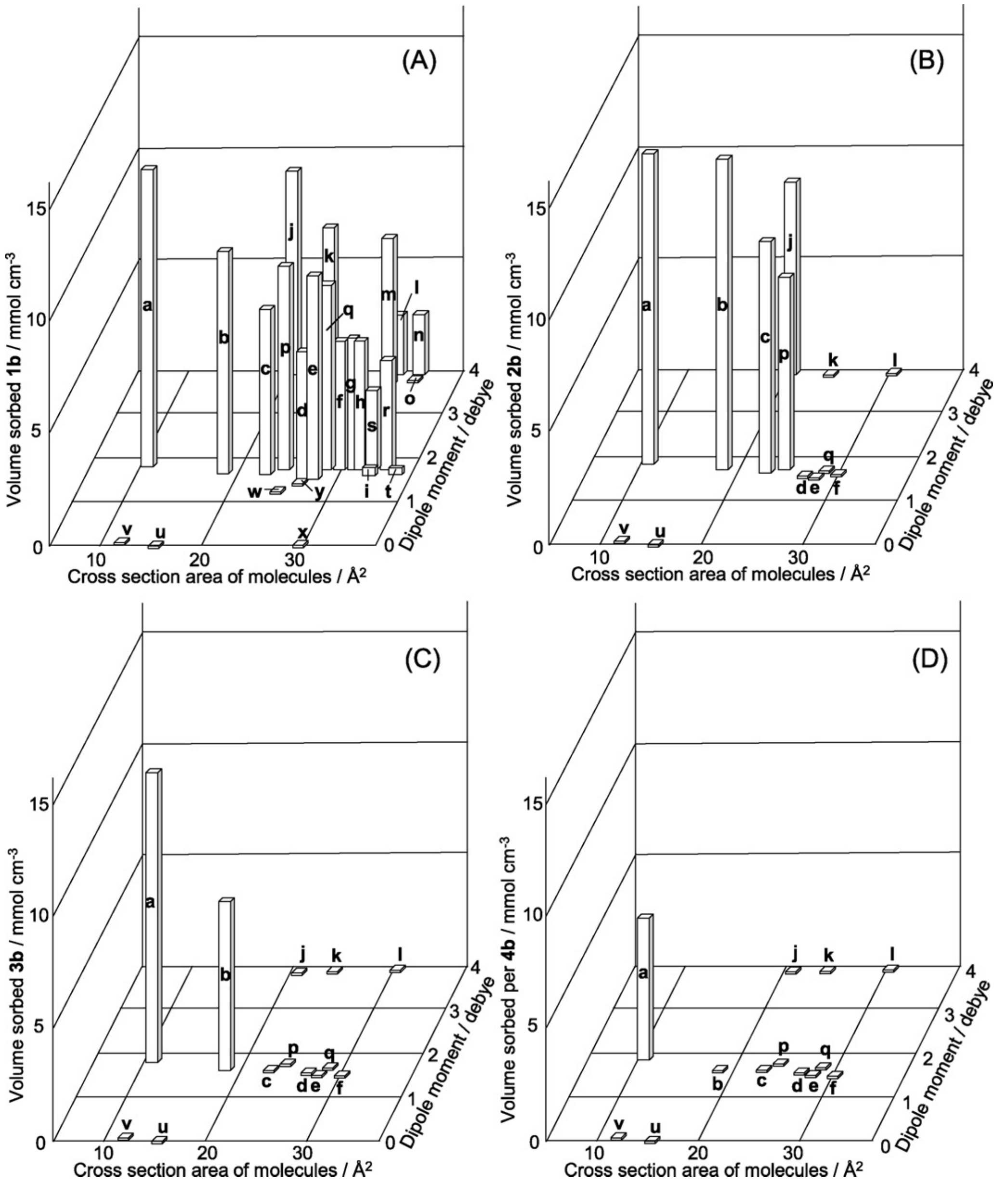

Fig. 4. Effects of the cross-section areas and the dipole moments of guest molecules on the sorption properties of **1b**–**4b** ($P/P_0 = 0.8$ at 298 K). (A) **1b**, (B) **2b**, (C) **3b**, and (D) **4b**. (a) Water, (b) methanol, (c) ethanol, (d) 1-propanol, (e) 2-propanol, (f) 1-butanol, (g) 2-butanol, (h) *iso*-butanol, (i) *tert*-butanol, (j) acetonitrile, (k) propionitrile, (l) butylonitrile, (m) *iso*-butylonitrile, (n) valeronitrile, (o) benzonitrile (313 K), (p) methyl formate, (q) methyl acetate, (r) ethyl acetate, (s) methyl propionate, and (t) ethyl propionate.

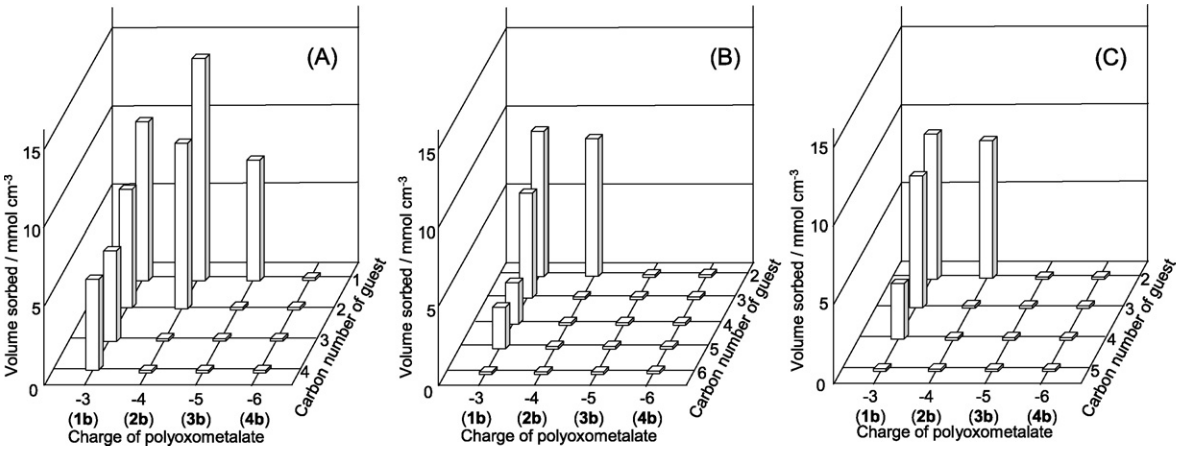

Fig. 5. Effects of the charges of the polyoxometalates on the amounts of sorption of polar organic molecules ($P/P_0 = 0.8$ at 298 K). (A) Amounts of sorption of alcohols. C1–C4 guests are methanol, ethanol, 1-propanol, and 1-butanol, respectively. (B) Amounts of sorption of nitriles. C1–C4 guests are acetonitrile, propionitrile, butylonitrile, and valeronitrile, respectively. (C) Amounts of sorption of esters. C1–C4 guests are methylformate, methylacetate, methylpropionate, and ethylpropionate, respectively.

The water of crystallization in **1a**–**4a** was either in the vicinity of the alkali metal ion or hydrogen-bonded to the constituent ions (polyoxometalate and macrocation) or to the other water molecules. The water of crystallization in **1a**–**3a** was completely desorbed by the evacuation at room temperature, while about 50% of the water of crystallization in **4a** was desorbed. The respective **1a**–**4a** after the evacuation at room temperature were denoted by **1b**–**4b**. The observed XRD patterns of **1b**–**4b** were fairly well reproduced by the structures **1b**–**4b**, respectively, as shown in Ref. [48]. The structures **1b**–**4b** showed the close packing of the columns. The calculated cell volumes per formula (V/Z) decreased in the order of **1b** (1497 Å^3) > **2b** (1467 Å^3) > **3b** (1412 Å^3) > **4b** (1406 Å^3). The decrease in the cell volumes would be related to the increase in the anion-cation interactions because of the close packing of the constituent ions with increase in n of $[\alpha\text{-XW}_{12}O_{40}]^{n-}$ (X = Co, B, Si, P). The BET surface areas of **1b**–**4b** were small (<2 m^2 g^{-1}) in accord with the close packing of the columns where no micropores existed. The crystal structures of **1a**–**4a** were completely restored by the exposure of **1b**–**4b** to the saturated water vapor.

2.2. Selective sorption of small polar molecules

The compound **1b** reversibly sorbed various kinds of polar (hydrophilic) organic molecules such as alcohols, nitriles, and esters as well as water. Neither hydrophobic dichloromethane and dichloroethane nor molecules without or with small polarity such as nitrogen monoxide, dinitrogen, and methane were sorbed despite the small sizes. The compound **2b** sorbed water, methanol, ethanol, acetonitrile, and methyl formate. The compound **3b** sorbed water and methanol, and **4b** sorbed only water. Fig. 4A–D show effects of molecular sizes and dipole moments of guest molecules on the sorption properties of **1b**–**4b** ($P/P_0 = 0.8$, 298 K). The sorption properties of **1b**–**4b** depended on not only the molecular sizes but also the dipole moments.

Fig. 5A–C show effects of the charges of the polyoxometalates on the amounts of sorption of alcohols, nitriles, and esters. The compounds **1b**–**3b** sorbed alcohols up to C4 (1-butanol), C2 (ethanol), and C1 (methanol), respectively, and **4b** sorbed no alcohols. The compound **1b** sorbed nitriles up to C5 (valeronitrile) while **2b** sorbed only acetonitrile (C2), and **3b** and **4b** excluded even acetonitrile. The compound **1b** sorbed esters up to methyl propionate (C4) while **2b** sorbed only methyl formate, and **3b** and **4b** excluded even methyl formate. Thus, polar small organic molecules such as alcohols, nitriles, and esters (≤C5) could be discriminated with **1b**–**4b**, and the increase in n of $[\alpha\text{-XW}_{12}O_{40}]^{n-}$ enabled the sorption of molecules with the shorter methylene chain. The sorption properties of **1b**–**4b** were applied to the separation of molecules of mixtures of alcohols, nitriles, and esters as reported in Refs. [42,44,48]. Such selectivity has not been reported for zeolites, coordination polymers, and layered compounds, and the sorption properties of **1b**–**4b** were compared with the other compounds in Table 1. The amounts of water and small alcohol sorption per volume were comparable to or larger than the other compounds while the amounts per weight were smaller due to the larger density of **1b**–**4b** (3.75–4.83 cm^3 g^{-1}).

2.3. Nature of sorption property

The nature of the sorption by the ionic crystal of **1b** can be explained as follows: since the structures of **1b** showed the close packing of the constituent ions, the lattice volumes of **1b** need to increase with the sorption. As shown in Fig. 6, the energy needed for the lattice expansion (E_1, which is a positive value) is compensated by the ion-dipole and hydrogen bonding interactions between the alcohols and **1b** (E_{int}, which is a negative value). If the absolute value of E_{int} is larger than E_1, the alcohols can be sorbed into the solid bulk. E_{int} is proportional to the dipole moment of the alcohol and inversely proportional to the ion-dipole (host-guest) distance. The dipole moments of C1–C4 alcohols (1.59–1.70 debye) are almost independent of the number of carbon atoms while the sizes (4.78–6.34 Å in diameter) increase with the number of carbon atoms (Fig. 4A).

Table 1
Amounts of water and small alcohol sorption for various compounds (mmol/cm^3) ((mmol/g))[a,b]

Compound	Water	Methanol	Ethanol	Propanol	Reference
Zeolites					
1. Na-Y (Si/Al = 2.47)[c]	–	9.8 (7.0)	7.0 (5.0)	5.6 (4.0)	[50]
2. ZSM-5 (Si/Al = 990)[d]	–	5.7 (3.3)	4.7 (2.7)	4.2 (2.4)	[51]
3. 3A[e]	9.2 (4.9)	–	0.1 (0.1)	–	[52]
4. 5A[f]	13 (7.7)	–	1.2 (0.7)	–	[52]
MOF or coordination polymers					
5. $[CoT(p\text{-}CO_2)PPCo_{1.5}(C_5H_5N)_3(H_2O)]$[g]	29 (15)	2.9 (1.5)	2.1 (1.1)	1.8 (0.9)	[53]
6. $[Ni(C_{20}H_{32}N_8)][C_6H_9(COOH)_2(COO)]_2\cdot 4H_2O$[b]	–	8.5 (6.4)	5.7 (4.3)	–	[54]
7. $[Ni(C_{20}H_{32}N_{83})][C_6H_9(COO)_3]_2\cdot 16H_2O$[b]	–	14 (12)	11 (9.3)	–	[54]
8. $[Ni_2(4,4'\text{-bipyridine})_3(NO_3)_4]\cdot 2C_2H_5OH$[b]	–	6.1 (4.5)	3.1 (2.3)	–	[55]
9. $[Ni_2(4,4'\text{-bipyridine})_3(NO_3)_4]\cdot 2CH_3OH$[b]	–	4.2 (3.3)	5.8 (2.7)	–	[55]
10. $[Ni_2(C_{26}H_{52}N_{10})]_3(btc)_4\cdot 4H_2O$[h]	–	12 (11)	6.3 (5.7)	2.5 (2.2)[i]	[56]
11. $[NiL]_3(btc)_2\cdot 14H_2O$[b,j]	–	–	1.4 (1.2)	–	[57]
12. $[Cu(\text{iso nicotinate})_2]$[b]	–	5.0 (3.3)	7.9 (3.3)	3.5 (2.4)	[58]
13. $Zn_2(btc)(NO_3)\cdot(H_2O)(C_2H_5OH)_5$[b,h]	–	–	9.6 (11)	–	[59]
14. $[Gd(imidc)_2(H_2O)_3](H_2O)$[b,k]	13.8 (5.0)	0.0 (0.0)	–	–	[60]
15. $Tb(bdc)(NO_3)\cdot 2[(CH_3)_2CONH]$[b,l]	–	7.2 (5.2)	5.4 (3.9)	3.6 (2.6)[i]	[61]
16. $[Tb(H_2L)_3]\cdot 2H_2O$[m]	4.0 (2.3)	1.8 (1.0)	0.0 (0.0)	–	[62]
17. $[K_2Mg_2\{U_2(C_2O_4)_7\}\cdot 2H_2O]\cdot 9H_2O$[b]	–	3.0 (1.4)	2.3 (1.0)	–	[63]
Layered compounds					
18. Montmorillonite[b,n]	16 (8.0)	7.3 (3.6)	5.5 (2.7)	5.9 (2.9)	[64]
19. $VOPO_4\cdot 2H_2O$[b]	–	12 (6.2)	12 (6.2)	5.8 (3.1)	[65]
Polyoxometalate compounds					
20. $(NH_4)_3PW_{12}O_{40}$	–	2.7 (0.9)	2.1 (0.7)	2.0 (0.7)	[51]
21. $Na_2[Cr_3O(OOCH)_6(H_2O)_3][\alpha\text{-}PW_{12}O_{40}]$	18 (4.7)	10 (2.7)	7.0 (1.9)	6.7 (1.8)	[48]
22. $K_3[Cr_3O(OOCH)_6(H_2O)_3][\alpha\text{-}SiW_{12}O_{40}]$	18 (4.6)	18 (4.6)	10 (2.7)	0.0 (0.0)	[48]
23. $Rb_4[Cr_3O(OOCH)_6(H_2O)_3][\alpha\text{-}BW_{12}O_{40}]$	19 (4.4)	9.5 (2.2)	0.0 (0.0)	0.0 (0.0)	[48]
24. $Cs_5[Cr_3O(OOCH)_6(H_2O)_3][\alpha\text{-}CoW_{12}O_{40}]$	6.5 (1.4)	0.0 (0.0)	0.0 (0.0)	0.0 (0.0)	[48]
25. $K_2[Cr_3O(OOCC_2H_5)_6(H_2O)_3]_2[\alpha\text{-}SiW_{12}O_{40}]$	3.4 (1.1)	7.5 (2.5)	5.0 (1.7)	1.6 (0.6)	[48]
26. $[\text{Calix[4]arene-Na}]_3[\alpha\text{-}PW_{12}O_{40}]$	1.9 (0.8)	3.9 (1.7)	1.9 (0.8)	–	[39]

[a] Figures show the amount in (mmol/cm^3) (amount per volume of desolvated compound). Figures in parenthesis show the amount in (mmol/g) (amount per gram of desolvated compound).

[b] Cell volume of the solvated phase is used for the calculation since that of the desolvated phase is unknown.

[c] $Na_{55.3}Al_{55.3}Si_{136.7}O_{384}$.

[d] $Si_{92}O_{192}$.

[e] $K_{12}Al_{12}Si_{12}O_{48}$.

[f] $Ca_6Al_{12}Si_{12}O_{48}$.

[g] TPP: tetraphenylporphyrin.

[h] btc: benzenetricarboxylate.

[i] Amount of isopropanol.

[j] L: 3,10-bis(2-ethyl)-1,3,5,8,10,12-hexaazacyclotetradecane.

[k] imidc: 4,5-imidazoledicarboxylate.

[l] bdc: benzenedicarboxylate.

[m] L: (***S***)-$O_3PCH_2NC_4H_7CO_2$.

[n] $(NaCa)_{0.3}(AlMg)_2Si_4O_{10}(OH)_2$.

Therefore, the absolute values of E_{int} do not change significantly with the increase in the number of carbon atoms [66]. On the other hand, the volumes of alcohols are proportional to third power of the sizes and increase with the increase in the number of carbon atoms, resulting in the increase in E_1. Therefore, the absolute value of E_{int} becomes smaller than E_1 at a certain alcohol (*tert*-butanol) and **1b** sorbs alcohols up to 1-butanol.

E_1 much increases with the increase in n of $[\alpha\text{-}XW_{12}O_{40}]^{n-}$ (from **1b** to **4b**); for example, 18, 37, 67, and 104 kJ mol^{-1} for the sorption of methanol by **1b**–**4b**, respectively. On the other hand, the absolute values of E_{int} do not change significantly because the number of the alkali metal, which can work as a sorption site in addition to the macrocation and the polyoxometalate, increases from 2 (**1b**) to 5 (**4b**) while the ionic radii increase and the interaction is weakened [67]. Therefore, the difference in the absolute values of E_{int} and E_1 decreases from **1b** to **4b** and the upper limit of the number of carbon atoms of alcohols sorbed into the bulk of **1b**–**4b** decreases with n [43,48].

3. Ionic crystals with both hydrophilic and hydrophobic channels

3.1. Syntheses and crystal structures

The ionic crystals **1a–4a/1b–4b** with the macrocation of $[Cr_3O(OOCH)_6(H_2O)_3]^+$ possessed only hydrophilic channels

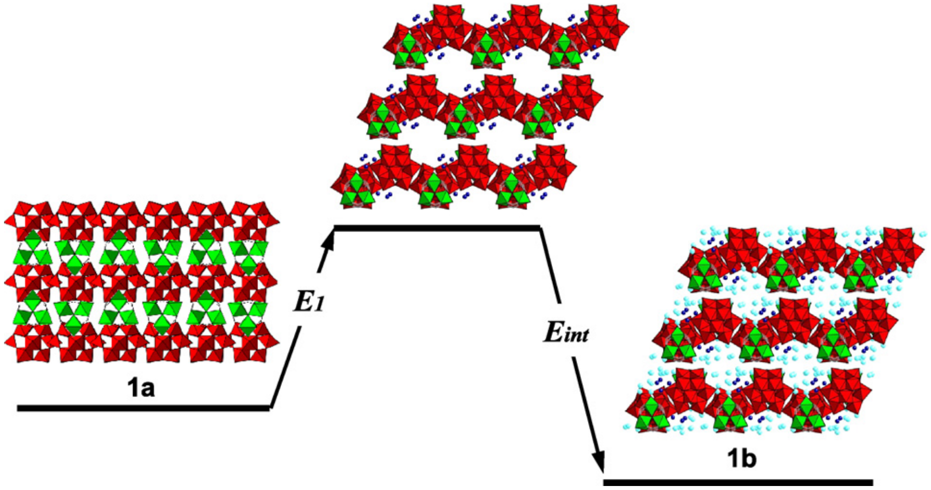

Fig. 6. Schematic model of the energy changes in the guest sorption.

in the crystal lattice. Therefore, the complexation of macrocation of $[Cr_3O(OOCC_2H_5)_6(H_2O)_3]^+$ with the Keggin-type $[\alpha\text{-}SiW_{12}O_{40}]^{4-}$ polyoxometalate was attempted [47]. Fig. 7 shows the schematic illustration of the synthesis and crystal structure of $K_2[Cr_3O(OOCC_2H_5)_6(H_2O)_3]_2[\alpha\text{-}SiW_{12}O_{40}]\cdot 3H_2O$ [**5a**]. The compound **5a** was composed of layers running along the *ac*-plane, the layers were stacked along the *b* axis, and K^+ resided between adjacent layers. Straight channels surrounded by propionate ligands of macrocations ran along the *a*-axis between the two layers and no water of crystallization was found. The opening of the channel was ca. 2.5 × 5.1 Å. On the other hand, winding hydrogen bond networks of the water of crystallization existed along the [1 1 0] direction through the layers. The narrowest and widest opening of the hydrophilic network channel was ca. 2.5 Å and 4.3 Å, respectively. The water of crystallization in **5a** was completely desorbed by the evacuation to form guest free phase **5b**. Single crystal structure analyses of **5b** showed that the crystal structure was essentially the same with **5a**. Hereafter, the straight channel surrounded by the propionate ligands of the macrocation is designated as hydrophobic channel and the winding channel containing the water of crystallization is designated as the hydrophilic channel.

3.2. Sorption of ethanol in hydrophilic and hydrophobic channels

The guest sorption property of **5b** was investigated, and it was found that **5b** sorbed various kinds of hydrophilic and amphiphilic molecules such as water, alcohols, esters, and nitriles. The amounts of sorption of C1–C3 alcohols were larger than that of water. Neither hydrophobic dichloromethane and dichloroethane nor molecules without or with small polarity such as nitrogen monoxide, dinitrogen, and methane were sorbed despite the small sizes. The compound **5b** showed the amphiphilic sorption property, while $K_3[Cr_3O(OOCH)_6(H_2O)_3][\alpha\text{-}SiW_{12}O_{40}]$ [**2b**], sorbed only water and methanol under the same conditions.

The changes in the amounts of water sorption for **5b** ($P/P_0 = 0.60$) as a function of time are shown in Fig. 8. The amount gradually increased and was almost leveled off after 200 s. The water sorption could be reproduced by the linear driving force mass transfer model,

$$M_t = M_e\{1 - \exp(-k_1 t)\} \tag{1}$$

where M_t and M_e are the amounts of sorption at time t and equilibrium, respectively, and k_1 is the rate constant [55].

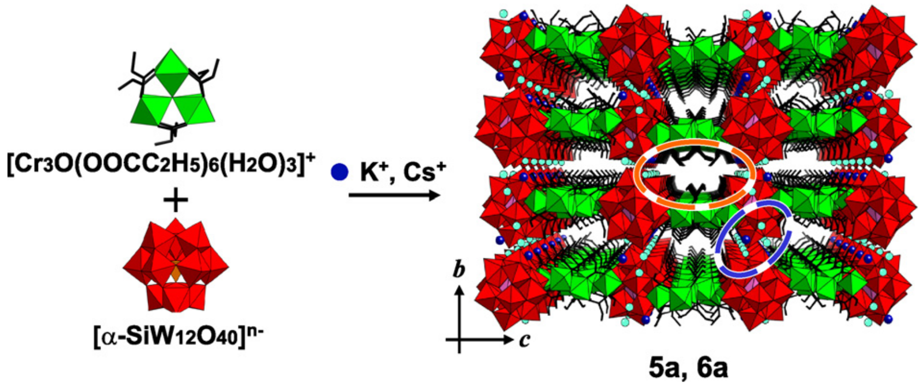

Fig. 7. Syntheses of ionic crystals with hydrophilic and hydrophobic channels.

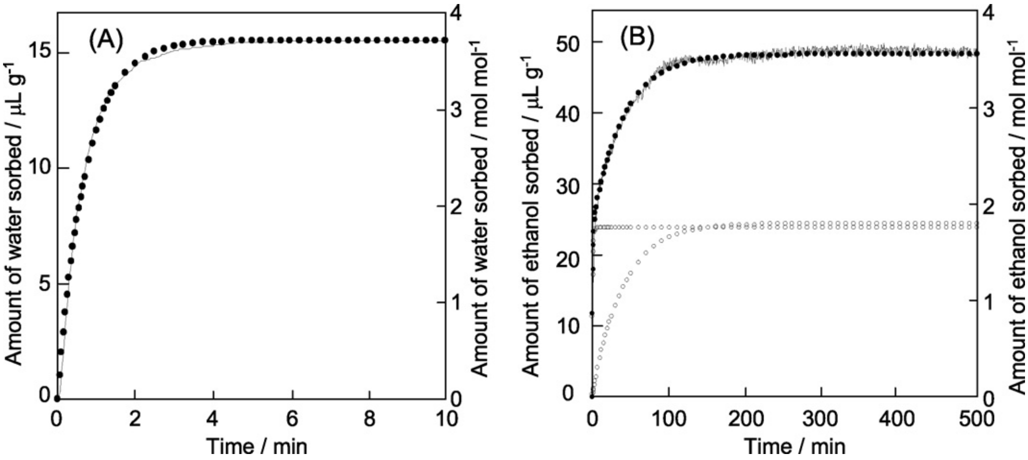

Fig. 8. Changes in the amounts of (A) water and (B) ethanol sorption for **5b** at 303 K as a function of time ($P/P_0 = 0.60$). The solid line shows the experimental data and solid circles show the calculated data according to the equation. Open circles show the two components for the calculation.

$M_e = 15.6\ \mu L\ g^{-1}$ ($3.71\ mol\ mol^{-1}$) and $k_1 = 2.3 \times 10^{-2}\ s^{-1}$ gave the best fit for the water sorption in Fig. 8A. In contrast, rapid sorption was initially observed and then the amount gradually increased for the ethanol sorption ($P/P_0 = 0.60$) as shown in Fig. 8B, and the profile could not be reproduced by Eq. (1). Therefore, two kinds of barriers were considered according to Eq. (2), as in the case of the alcohol sorption for the Ni-bipyridine compound [55].

$$M_t = M_{e1}\{1 - \exp(-k_1 t)\} + M_{e2}\{1 - \exp(-k_2 t)\} \quad (2)$$

where M_{e1} and M_{e2} are the contributions of the each of the two processes controlling the overall sorption (i.e., $M_{e1} + M_{e2} = M_e$: amounts of sorption at equilibrium), and k_1 and k_2 are the rate constants. The best fits for the ethanol sorption were given by $M_{e1} = 22.2\ \mu L\ g^{-1}$ ($1.63\ mol\ mol^{-1}$), $k_1 = 2.2 \times 10^{-2}\ s^{-1}$, $M_{e2} = 22.9\ \mu L\ g^{-1}$ ($1.68\ mol\ mol^{-1}$), and $k_2 = 4.2 \times 10^{-4}\ s^{-1}$ (Fig. 8B). The two processes probably describe the sorption into the hydrophilic and hydrophobic channels. In the *in situ* IR spectra (ν(OH) region: 3000–3600 cm^{-1}) of ethanol sorbed in **5b**, two bands at 3290 cm^{-1} and 3470 cm^{-1} appeared, which were assigned to ν(OH) bands of ethanol in the hydrophilic channel and hydrophobic channel, respectively. The 3290 cm^{-1} band intensity steeply increased with the increase in the ethanol vapor pressure and did not much increase above ca. $P/P_0 = 0.4$, while the 3470 cm^{-1} band intensity gradually increased with the increase in the ethanol vapor pressure and steeply increased around $P/P_0 = 0.5$. Therefore, ethanol are mainly sorbed into the hydrophilic channel at the low vapor pressure, while the sorption into the hydrophobic channel was dominant above $P/P_0 = 0.5$.

3.3. Channel-selective sorption and collection of hydrophilic and hydrophobic molecules

In the crystal structure of **5b**, K^+ resided between the layers, and the change of K^+ to larger Cs^+ would increase the interlayer distance and the opening of the hydrophobic channel. The opening and volume of the hydrophobic channel increased from 2.5 Å × 5.1 Å and 23 µL in **5b** to 4.0 Å × 5.2 Å and 30 µL in $Cs_2[Cr_3O(OOCC_2H_5)_6(H_2O)_3]_2[\alpha\text{-}SiW_{12}O_{40}]$ [**6b**] [49]. The guest sorption property of **6b** was investigated at 298 K. The compound **6b** sorbed various kinds of hydrophilic molecules such as water and alcohols as well as hydrophobic molecules such as dichloromethane and dichloroethane. The amount of dichloromethane reached 23 $\mu L\ g^{-1}$ ($1.6\ mol\ mol^{-1}$) at $P/P_0 = 0.94$. The changes in the amounts of dichloromethane sorption by **6b** as a function of time were reproduced with a single rate constant, showing that a single barrier existed for the sorption. The amount of dichloromethane sorption by **6b** at $P/P_0 = 0.60$ (298 K) upon the pre-sorption of water ($22 \pm 1\ \mu L\ g^{-1}$, $5.5 \pm 0.2 H_2O$ per **6b**) was $9.3 \pm 0.5\ \mu L\ g^{-1}$ ($0.66 \pm 0.03 CH_2Cl_2$ per **6b**) and fairly agreed with that $10 \pm 0.5\ \mu L\ g^{-1}$ without the pre-treatment. The opening of the hydrophobic channel in **6b** (4.0 Å × 5.2 Å) was comparable to the diameter of the dichloromethane molecule (4.2 Å). These facts show that dichloromethane is accommodated into the hydrophobic channel in **6b** and that the amount is not influenced by the pre-sorption of water.

When **6b** was exposed to a gas flow (He balance) containing water ($P/P_0 = 0.60$) and dichloromethane ($P/P_0 = 0.40$), the weight increased as shown in Fig. 9. The best fits for the experimental data were given by $k_1 = 1.7 \times 10^{-2}\ s^{-1}$, $M_{e1} = 16.4\ \mu L\ g^{-1}$ (1.64 wt%), $k_2 = 3.0 \times 10^{-3}\ s^{-1}$, and $M_{e2} = 7.0\ \mu L\ g^{-1}$ (0.93 wt%). The k_1 and M_{e1} values were close to those of water sorption at $P/P_0 = 0.60$ and the k_2 and M_{e2} values were close to those of dichloromethane sorption at $P/P_0 = 0.40$. Therefore, the rate and equilibrium amount of the dichloromethane sorption into the hydrophobic channel and those of water into the hydrophilic channel of **6b** were independent of each other, and the phenomenon was different from those of zeolites and activated carbons, of which the amounts of dichloromethane sorption are decreased by the presence of water [68].

The collection of dichloromethane and water from the gas mixture was attempted with **6b** according to Scheme 1. Compound **6a** was evacuated at 298 K for 6 h to form **6b** followed by the exposure to the gas mixture of water ($P/P_0 = 0.85$) and dichloromethane ($P/P_0 = 0.71$) at 298 K for

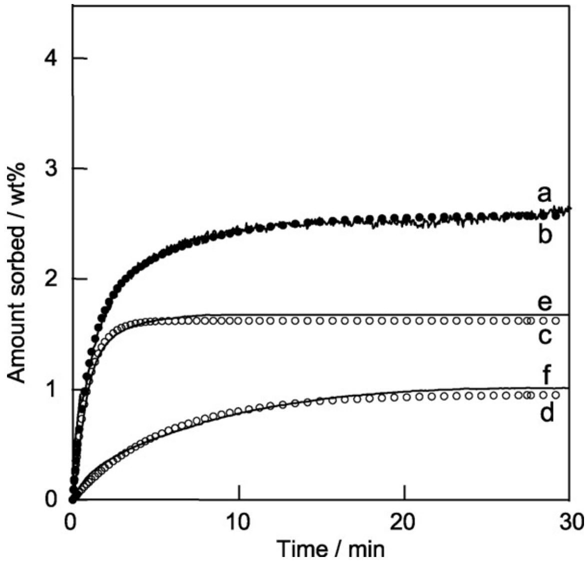

Fig. 9. Changes in the weight of **6b** by the exposure to a gas mixture of water ($P/P_0 = 0.60$) and dichloromethane ($P/P_0 = 0.40$) at 298 K. Solid line (a) shows the experimental data. Solid lines (e) and (f) show the experimental sorption data of water ($P/P_0 = 0.60$) and dichloromethane ($P/P_0 = 0.40$), respectively. Solid circle (b) shows the calculated data, and open circles (c) and (d) show the two components for the calculation.

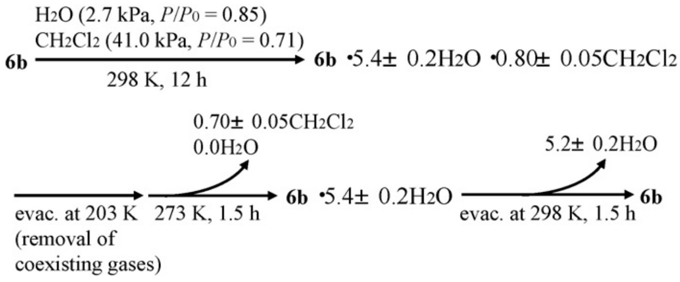

Scheme 1.

12 h to form **6b**·$5.4 \pm 0.2H_2O$·$0.8 \pm 0.05CH_2Cl_2$. After the removal of the coexisting gases, the sample was heated at 273 K and kept for 1.5 h. The amount of dichloromethane evolved was $9.9 \pm 0.5\ \mu L\ g^{-1}$ ($0.70 \pm 0.05CH_2Cl_2$ per **6b**). Then the sample was evacuated at 298 K for 1.5 h and the amount of water collected was $22 \pm 1\ \mu L\ g^{-1}$ ($5.2 \pm 0.2H_2O$ per **6b**). Thus, dichloromethane and water sorbed in **6b** were successfully collected.

4. Conclusion

This review described our recent studies on the design and syntheses ionic crystals of polyoxometalates, macrocations, and alkali metal ions with hydrophilic/hydrophobic channels and the selective sorption properties. The followings are the future goals to be achieved: (1) separation of azeotropic mixtures and close-boiling mixtures: systematic change of the size, shape, hydrophilicity/hydrophobicity of the molecular-sized spaces in the ionic crystals would control the interaction between the guest molecules and the solid hosts, leading to the separation and collection of mixtures. The target separations are water/alcohol, alkane/alkene, stereo-isomers, etc. (2) Catalysis in the ionic crystals: polyoxometalates catalyze oxidation or acid-base reactions, and the catalytic properties can be controlled at atomic or molecular levels. Complexation of polyoxometalates with macrocations would work as heterogeneous catalysts. Moreover, a unique reaction would proceed in the molecular-sized space or by the cooperation with the macrocation.

Acknowledgements

This work was supported in part by the Core Research for Evolutional Science and Technology (CREST) program of the Japan Science and Technology Agency (JST) and Grant-in-Aid for Scientific Research from the Ministry of Education, Culture, Sports, Science, and Technology of Japan.

References

[1] M.E. Davis, Nature 417 (1992) 813.
[2] A. Corma, F. Rey, S. Valencia, J.L. Jorda, J.A. Rius, Nature Mater. 2 (2003) 493.
[3] S.M. Kuznicki, V.A. Bell, H.W. Hillhouse, R.M. Jacubinas, C.M. Braunbarth, B.H. Toby, M. Tsapatsis, Nature 412 (2001) 720.
[4] S.M. Csicsery, Pure Appl. Chem. 58 (1986) 841.
[5] P.B. Weisz, V.J. Frilette, J. Phys. Chem. 64 (1962) 382.
[6] S. Kitagawa, R. Kitaura, S. Noro, Angew. Chem. Int. Ed. 43 (2004) 2334.
[7] M. Eddaoudi, D.B. Moler, H. Li, B. Chen, T.M. Reineke, M. O'Keeffe, O.M. Yaghi, Acc. Chem. Res. 34 (2001) 319.
[8] H.L. Ngo, W. Lin, Top. Catal. 34 (2005) 85.
[9] G. Férey, C. Mellot-Draznieks, C. Serre, F. Millange, J. Dutour, S. Surblé, I. Margiolaki, Science 309 (2005) 2040.
[10] K. Takaoka, M. Kawano, T. Hozumi, S. Ohkoshi, M. Fujita, Inorg. Chem. 45 (2006) 3976.
[11] F. Cavani, F. Trifiro, A. Vaccari, Catal. Today 11 (1991) 173.
[12] R. Burch (Ed.), Catal. Today 2 (1988) 185, Special issue on pillared clays.
[13] H. Cölfen, M. Antonietti, Angew. Chem. Int. Ed. 44 (2005) 5576.
[14] M. Eddaudi, J. Kim, N. Rosi, D. Vodak, J. Wachter, M. O'Keeffe, O.M. Yaghi, Science 295 (2002) 469.
[15] R. Matsuda, R. Kitaura, S. Kitagawa, Y. Kubota, R.V. Belosludov, T.C. Kobayashi, H. Sakamoto, T. Chiba, M. Takata, Y. Kawazoe, Y. Mita, Nature 436 (2005) 238.
[16] S. Yamanaka, F. Kanamaru, M. Koizumi, J. Phys. Chem. 78 (1974) 42.
[17] S. Piana, M. Reyhani, J.D. Gale, Nature 438 (2005) 70.
[18] M.T. Pope, A. Müller, Angew. Chem., Int. Ed. Engl. 30 (1991) 34.
[19] C.L. Hill, C.M. Prosser-McCartha, Coord. Chem. Rev. 143 (1995) 407.
[20] T. Okuhara, N. Mizuno, M. Misono, Adv. Catal. 41 (1996) 113.
[21] C.L. Hill (Ed.), Chem. Rev. 98 (1998) 1, Special issue on polyoxometalate.
[22] T. Yamase, M.T. Pope (Eds.), Polyoxometalate Chemistry for Nano-Composite Design, Kluwer, Dordrecht, The Netherlands, 2002.
[23] I.V. Kozhevnikov, Catalysis by Polyoxometalates, Wiley, Chichester, UK, 2002.
[24] R. Neumann, in: J.E. Bäckvall (Ed.), Oxidation Methods, Wiley-VCH, Weinheim, 2004, p. 223.
[25] N. Mizuno, K. Kamata, K. Yamaguchi, Surface and Nanomolecular Catalysis, Taylor and Francis Group, LLC, New York, 2006, p. 463.
[26] D.L. Long, P. Kogerler, L.J. Farrugia, L. Cronin, Chem. Asian. J. 1 (2006) 352.
[27] N. Mizuno, M. Misono, Chem. Lett. (1987) 967.
[28] T. Ito, K. Inumaru, M. Misono, J. Phys. Chem. B 101 (1997) 9958.
[29] T. Okuhara, H. Watanabe, T. Nishimura, K. Inumaru, M. Misono, Chem. Mater. 12 (2000) 2230.
[30] A. Müller, S.Q.N. Shah, H. Bögge, M. Schmidtmann, Nature 397 (1999) 48.
[31] T. Yamase, P.V. Prokop, Angew. Chem. Int. Ed. 41 (2002) 466.

[32] M. Hölscher, U. Englert, B. Zibrowius, W.F. Hölderich, Angew. Chem. Int. Ed. Engl. 33 (1994) 2491.
[33] M.I. Khan, E. Yohannes, D. Powell, Inorg. Chem. 38 (1999) 212.
[34] D. Hagrman, P.J. Hagrman, J. Zubieta, Angew. Chem. Int. Ed. 38 (1999) 3165.
[35] J.H. Son, H. Choi, Y.U. Kwon, J. Am. Chem. Soc. 122 (2000) 7432.
[36] C. Du Peloux, A. Dolbecq, P. Mialane, J. Marrot, E. Rivière, F. Sécheresse, Angew. Chem. Int. Ed. 40 (2001) 2455.
[37] A. Forment-Aliaga, E. Coronado, M. Feliz, A. Gaita-Ariño, R. Llusar, F.M. Romero, Inorg. Chem. 42 (2003) 8019.
[38] M.V. Vasylyev, R. Neumann, J. Am. Chem. Soc. 126 (2004) 884.
[39] Y. Ishii, Y. Takenaka, K. Konishi, Angew. Chem. Int. Ed. 43 (2004) 2702.
[40] S.S. Mal, U. Kortz, Angew. Chem. Int. Ed. 44 (2005) 3777.
[41] H.A. An, E.B. Wang, D.R. Xiao, Y.G. Li, Z.M. Su, L. Xu, Angew. Chem. Int. Ed. 45 (2006) 904.
[42] S. Uchida, M. Hashimoto, N. Mizuno, Angew. Chem. Int. Ed. 41 (2002) 2814.
[43] S. Uchida, N. Mizuno, Chem.-Eur. J. 9 (2003) 5850.
[44] S. Uchida, N. Mizuno, J. Am. Chem. Soc. 126 (2004) 1602.
[45] S. Uchida, R. Kawamoto, T. Akatsuka, S. Hikichi, N. Mizuno, Chem. Mater. 17 (2005) 1367.
[47] R. Kawamoto, S. Uchida, N. Mizuno, J. Am. Chem. Soc. 127 (2005) 10560.
[48] S. Uchida, R. Kawamoto, N. Mizuno, Inorg. Chem. 45 (2006) 5136.
[49] C. Jiang, A. Lesbani, S. Uchida, R. Kawamoto, N. Mizuno, J. Am. Chem. Soc. 128 (2006) 14240.
[50] B. Sulikowski, J. Phys. Chem. 97 (1993) 1420.
[51] V.S. Nayak, J.B. Moffat, J. Phys. Chem. 92 (1988) 7097.
[52] E. Lalik, R. Mirek, J. Rakoczy, A. Groszek, Catal. Today 114 (2006) 242.
[53] M.E. Kosal, J.H. Chou, S.R. Wilson, K.S. Suslik, Nature Mater. 1 (2002) 118.
[54] K.S. Min, M.P. Suh, Chem. Eur. J. 7 (2001) 303.
[55] A.J. Fletcher, E.J. Cussen, D. Bradshaw, M.J. Rosseinsky, K.M. Thomas, J. Am. Chem. Soc. 126 (2004) 9750.
[56] M.P. Suh, J.W. Ko, H.J. Choi, J. Am. Chem. Soc. 124 (2002) 10976.
[57] T.B. Lu, H. Xiang, R.L. Luck, L. Jiang, Z.W. Mao, L.N. Ji, New. J. Chem. 26 (2002) 969.
[58] J.Y. Lu, A.M. Babb, Chem. Commun. (2002) 1340.
[59] M. Eddaoudi, H. Li, O.M. Yaghi, J. Am. Chem. Soc. 122 (2000) 391.
[60] T.P. Maji, G. Mostafa, H.C. Chang, S. Kitagawa, Chem. Commun. (2005) 2436.
[61] T.M. Reineke, M. Eddaoudi, M. O'Keeffe, O.M. Yaghi, Angew. Chem. Int. Ed. 38 (1999) 2590.
[62] Q. Yue, J. Yang, G.H. Li, G.D. Li, J.S. Chen, Inorg. Chem. 45 (2006) 4431.
[63] I. Imaz, G. Bravic, J.P. Sutter, Chem. Commun. (2005) 993.
[64] C. Breen, A.T. Deane, J.J. Flynn, D. Reynolds, Clay Clay Miner. 35 (1987) 336.
[65] N. Yamamoto, N. Hiyoshi, T. Okuhara, Chem. Mater. 14 (2002) 3882.
[66] The E_1 values from **1b** to the guest included phases were 18, 26, 33, and 40 kJ mol^{-1} for 1 mol mol^{-1} of C1–C4 alcohols, respectively, and increased with the number of carbon atoms. On the other hand, assuming the ion-dipole interaction with the sodium ion (Na–O = 2.3 Å) or dipole-dipole interaction with the oxygen atom of the polyoxometalate or macrocation (O–O = 3.0 Å), the E_{int} values of 1 mol mol^{-1} of C1–C4 alcohols sorbed in **1b** were in the range of −63 to −68 kJ mol^{-1}, and did not change significantly with the increase in the number of carbon atoms.
[67] The E_1 values from **1b** to **4b** to the corresponding guest included phases for 1 mol mol^{-1} of methanol largely increased from 18 kJ mol^{-1} (**1b**) to 104 kJ mol^{-1} (**4b**). On the other hand, the E_{int} values of 1 mol mol^{-1} of methanol sorbed in **1b**–**4b** calculated in the same way as that in Ref. [66] were in the range of −50 to −68 kJ mol^{-1}, and did not change significantly.
[68] J.H. Yun, D.K. Choi, S.H. Kim, AIChE J. 44 (1998) 1344.